Computational Study of Effect of Nozzle Exit Shape on the Heat Transfer Rate in Impingement Jet Cooling

Vishnu Vijayaan, Rakesh P
Department of Mechanical Engineering
College of Engineering Trivandrum (CET)
Thiruvananthapuram,
vishnuvijayan7575@gmail.com
rakp73@gmail.com

Abstract— **For the work of this thesis the commercially available program package of FLUENT 6.3, and Gambit 2.4 is used for all the simulation and geometry generation tasks. All the nozzle inlet parameters like, Geometry (Diameter of nozzle, Distance b/w nozzle & surface), Shape of nozzle (Round nozzle, Rectangular nozzle and square nozzle) and a single plane jet and swirl jet are studied with the experimental reference available for each cases.**

The simulations were performed for three different geometries with plain jet at jet to plate spacing 0.5, 1, and 4; Reynolds number 5000, 10000 and 15000.simulation for swirl jet with round nozzle, jet to plate spacing 0.5 and Reynolds number 5000, 10000, 15000. The results are validated with both experimental. This study can provide useful information to the application of impinging jet heat transfer.

Keywords—jet impingement; nozzle to surface spacing; swirl jet; nusselt number;

I. INTRODUCTION

Due to high rates of localized heat transfer, impinging jet flows are employed in a wide variety of applications of practical interest, such as surface coating and cleaning, cooling of electronic components, metal cutting and forming, fire testing and building materials, turbine blade cooling, drying of textiles, paper and film materials, aircraft wing leading edge heating for anti-icing application, etc. Even though the flow geometry is simple in jet impingement heat transfer problems, the physics of the flow is very complex due to the shear layer development at the free jet and wall jet boundaries, boundary layer development at the impingement surface, and very high streamline curvature near the impingement location.

In the case of gas turbines, higher thermal efficiency can be obtained by increasing the temperature of the gases at the turbine inlet. However, the heat bearing capacity of the blade material imposes a practical limitation on the turbine inlet temperature. Therefore, in order to effectively use higher inlet temperatures, it becomes necessary to employ a cooling mechanism within the blades. Several patents in this area of technology are documented. Many such cooling mechanisms involve the use of jet impingement cooling in one variation or another. Most of these methods employ a circular jet operating in confined spaces, which is the focus of this study. The effects of design variables, such as nozzle geometry and size, nozzle configuration, location of exhaust ports, nozzle-to-impinged surface, and surface motion, roughness of the target plate and operating variables, such as cross-flow, turbulence intensity at nozzle exit, jet axis velocity on the fluid flow, and heat transfer, need to be characterized in detail for optimal design. The choice of turbulence models is also very crucial in numerical analysis of impinging jet heat transfer process specifically due to the over prediction of kinetic energy generation at the impingement region by various eddy-viscosity models.

Recently there are many computational as well as experimental investigations done on flat surfaces with different varieties of jet and geometric parameters. Most of the previous studies on jet impingement have been focused to the two dimensional plane jets and circular jet and not much information is available on the effect of different inlet geometries. Most of them did not have computations for turbulent flow due to lack of suitable turbulence model. Yuling Shi, M. B. Ray, and A. S. Mujumdar[1] Two turbulence models, namely the standard k-model and the RSM, were used to calculate the heat transfer under a semiconfined impinging slot jet for various flow and geometric parameters. Parameters used, jet diameter(6.2, 5 mm), jet to plate spacing ratio(6, 2.6), Reynolds no(11000, 10200), plate temperature(338,348), jet temperature(375,310) respectively. Although both the models slightly over predicted the Nusselt number distributions under some conditions, the qualitative trends compared very well with the experimental trend in most cases. The simulated results compare favorably with the experimental results for large nozzle-to-target spacing, but the predictions for small nozzle-to-target spacing call for further improvement in the simulation. M.F. Koseoglu , S. Baskaya [2]experimentally and numerically investigated the influence of jet inlet geometry and aspect ratio on heat transfer characteristics of confined impinging jets .Experiments have been conducted for three different geometries and simulations were performed for nine different jet geometries at jet to plate distances of 2, 6, 12 circular jet

diameters. As the aspect ratio of equal cross-sectional area elliptic and rectangular jets increases, heat transfer enhancement in the stag nation region was obtained. As a result higher aspect ratio jets can be used as a passive enhancement technique for localized heating or cooling especially at small jet to plate distances.

II. PROBLEM DESCRIPTION

A. *Boundary conditions*

Fig.1 shows the schematic drawing of the confined impinging jet on a flat surface and the computational domain used for numerical simulation. Because of the symmetry, solutions were obtained for one quarter of the domain for 3D geometry.

In the present study three different nozzle geometries are selected with same exit area and the detailed dimensions are given in table.1. For all geometries simulations were performed for jet to plate spacing of 0.5,1,4 hydraulic diameter of jet with Reynolds number of 5000, 10000, 15000 for each case. The fluid considered is air and the temperature difference between jet and plate is 70^0C.

The boundary conditions used are, at the jet exit, velocity-inlet boundary condition is used with a velocity magnitude compatible to the jet-exit Reynolds number. A constant temperature at the jet exit is also specified. On the fiat surface, no-slip wall boundary condition with constant heat flux or isothermal is set. The confinement surface is considered to be an adiabatic wall, and the outlet is considered as fully developed outflow or constant pressure-outlet condition is used where the variables are extrapolated from inside. Turbulence intensity and length scale at the inlet for all the calculations were chosen to be 2% and 0.07 D (hydraulic diameter), respectively.

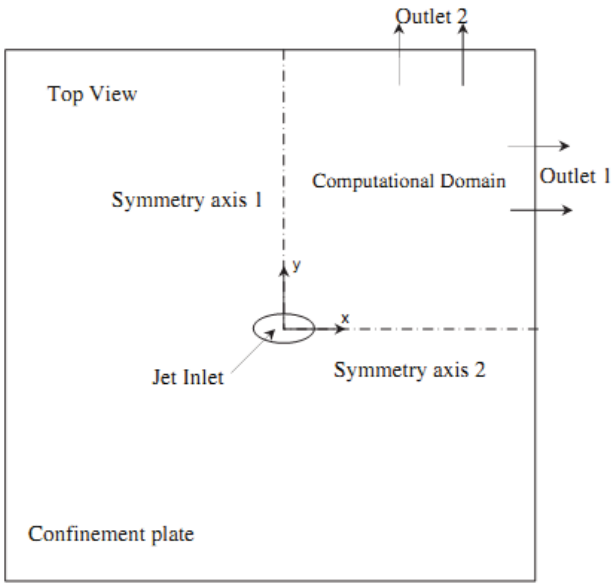

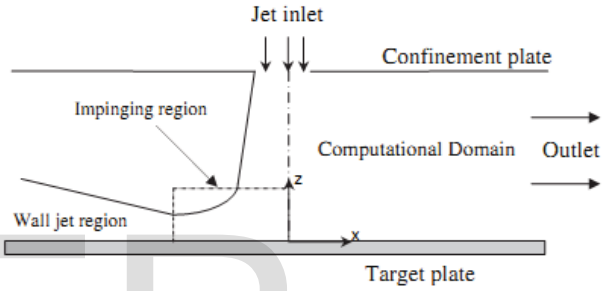

Fig. 1. Schematic diagram of jet impingement domain

B. *Numerical simulation*

The governing equations used are as follows:

Mass conservation equation

$$\frac{\partial U_i}{\partial x_i} = 0 \qquad (1)$$

Table 1. dimension of nozzle exit geometries

TYPE	BREADTH (mm)	HEIGHT (mm)	HYDRAULIC DIAMETER , d (mm)
Circular	20	20	20
Square	17.725	17.725	17.725
Rectangular	26	12	16.72

Momentum conservation equation

$$\rho U_j \frac{\partial U_i}{\partial U_j} = -\frac{\partial P}{\partial x_i} + \frac{\partial}{\partial x_j}\left(\mu \frac{\partial U_i}{\partial x_j} + \frac{\partial U_j}{\partial x_i}\right) - \overline{\rho u_i' u_j'} \qquad (2)$$

Energy conservation equation

$$\rho U_j \frac{\partial T_i}{\partial U_j} \frac{\partial}{\partial x_j}\left(\frac{\mu}{Pr}\frac{\partial T}{\partial x_j} - \overline{\rho T' u_j'}\right) \qquad (3)$$

Where,

P, T, and U_i are the mean pressure, temperature, and velocity components, respectively, T' and u_i' are the fluctuating temperature and velocity components, respectively x_i is the coordinate direction, and ρ, μ, and Pr are the fluid density, dynamic viscosity, and Prandtl number, respectively. The turbulent Reynolds stresses, $-\overline{\rho u_i' u_j'}$ in Eq. (2) are calculated by an appropriate turbulence model for closure. In the eddy-viscosity models, the turbulent stresses are assumed to be linearly proportional to the strain rate and are calculated as

$$-\overline{\rho u_i' u_j'} = \mu_t\left(\frac{\partial U_i}{\partial x_j} + \frac{\partial U_j}{\partial x_i}\right) - \frac{2}{3}\rho k \delta_{ij} \qquad (4)$$

Where μ_t is the turbulent eddy viscosity, δ_{ij} is the Kronecker delta and $k = \frac{u_i' u_i'}{2}$ is the kinetic energy of turbulence. The eddy viscosity, in turn, is obtained from an empirical formula as a function of the kinetic energy of turbulence and the turbulent length scale. In the standard k–ε model developed by Launder and Spalding the transport equations for the kinetic energy of turbulence, k, and the time rate of dissipation of k, which is defined as, $\varepsilon = (\frac{\mu}{\rho})(\partial u_i'/\partial x_j)(\partial u_i'/\partial x_j)$ are solved. The turbulent length scale, *l*, is related to k and ε as $l = k^{3/2}/\varepsilon$. Once k and ε are obtained from the solution of their respective transport equations, the eddy viscosity is calculated as $\mu_t = \rho C_\mu k^2/\varepsilon$ where C_μ is an empirical constant. The transport equations for k and ε are given as

$$\rho U_j \frac{\partial k}{\partial x_j} = \frac{\partial}{\partial x_j}\left(\left(\mu + \frac{\mu_t}{\sigma_k}\right)\frac{\partial k}{\partial x_j}\right) + P_k - \rho\varepsilon \quad (5)$$

$$\rho U_j \frac{\partial \varepsilon}{\partial x_j} = \frac{\partial}{\partial x_j}\left(\left(\mu + \frac{\mu_t}{\sigma_\varepsilon}\right)\frac{\partial \varepsilon}{\partial x_j}\right) + C_{1\varepsilon}\frac{\varepsilon}{k}P_k - C_{2\varepsilon}\rho\frac{\varepsilon^2}{k} \quad (6)$$

Where

$$P_k = (\mu_t\left(\frac{\partial U_i}{\partial x_j} + \frac{\partial U_j}{\partial x_i}\right) - \frac{2}{3}k\rho\delta_{ij})\frac{\partial U_i}{\partial x_j} \quad (7)$$

In these equations, P_k is the generations of turbulent kinetic energy due to the mean velocity gradients and buoyancy and the contribution of the fluctuating dilatation in compressible turbulence to the overall dissipation rate. $C_{1\varepsilon}$ and $C_{2\varepsilon}$, are constants and equal to 1.44, 1.92, respectively. σ_k=1.0 and σ_ε=1.3 are the turbulent Prandtl numbers for k and ε, respectively.

The geometries were created in GAMBIT software, impingement region is the most difficult domain to simulate accurately because of large gradients at streamline curvature. The grid layout in this region was specified to be much finer than that in the downstream region. A non-uniform grid was used in all the simulations, mesh size used was between 100K – 400K (K=10^3) and a typical grid distribution is shown in Figure 2.

.

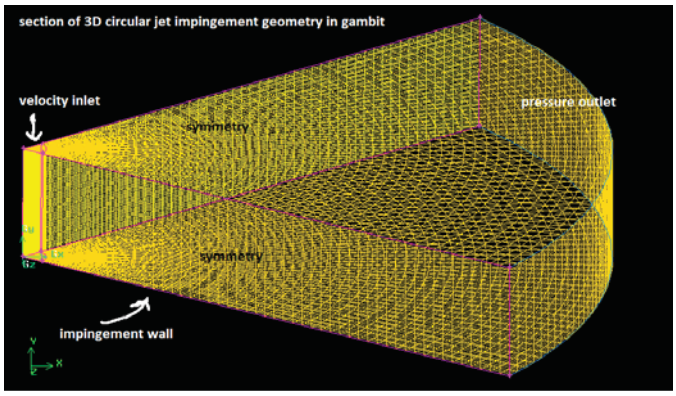

Fig. 2. Geometry and mesh created in GAMBIT

In this simulation work, CFD software FLUENT 6.3 was adopted. The governing equations are discretized using a second-order upwind interpolation scheme, and the discretized equations are solved using the SIMPLEC algorithm. The typical relaxation factors used were 0.3, 0.7, and 0.5 for pressure, momentum, and Reynolds stresses, respectively.

For energy and turbulent viscosity, the relaxation factors were 1, whereas a factor of 0.8 was used for the turbulent kinetic energy and turbulent energy dissipation rate. The solutions was considered converged when the normalized energy residual was less than 10^{-6} and the normalized residuals of all the other variables were less than 10^{-4}

III. RESULTS AND DISCUSSIONS

A. PLAIN JET

The effect of shape of the nozzle on the local Nusselt number distribution at Reynolds number of 5000, 10000 and 15000 for nozzle-to-plate spacing (z/d) of 0.5,1,2 are studied numerically. Figures 3-5 show the local distribution of Nusselt numbers along the horizontal line through the stagnation point for nozzles of three different cross sections, viz. circular, square and rectangular. One available experimental data [4] of the jet impingement flow were selected from the available literature as a comparison case

Local Nusselt number distributions at z/d = 0.5 are shown in Fig. 3 It is observed that with increase in the Reynolds numbers, Nusselt number increases at all radial locations for all the three nozzle configurations. This may be due to increase of the momentum of jet with Reynolds number. The stagnation Nusselt numbers for square and circular nozzles are almost same at all Reynolds numbers. Computational plot shows the exact behavior as in the experimental one.

Fig. 4 shows the distribution of local Nusselt numbers for all the three nozzles at z/d = 1. The trends are similar to the one observed at z/d = 0.5, but the stagnation values for rectangular nozzle case do not vary as much as at z/d = 0.5. However, the locations of secondary peaks shift away from the stagnation point.

Fig. 5 shows the distribution of local Nusselt numbers for various Reynolds number at z/d = 4. However, the stagnation point Nusselt number values are almost same for all the three nozzles for a particular Reynolds number.

From fig, 3,4,5 for a particular value of Reynolds number, Nusselts number value decreases with increase in nozzle to target plate spacing(H).This results from the increase of fluid velocity along the plate as H decreases.

On comparing the results obtained with the experimental data [4], there is a large difference in the values of Nusselts number distribution. The difference may be due to the restrictions in the numerical study, as we considered uniform flow distribution and constant turbulence intensity at the exit of all the nozzles. In the experimental study, turbulent intensity varies with shape of nozzle.

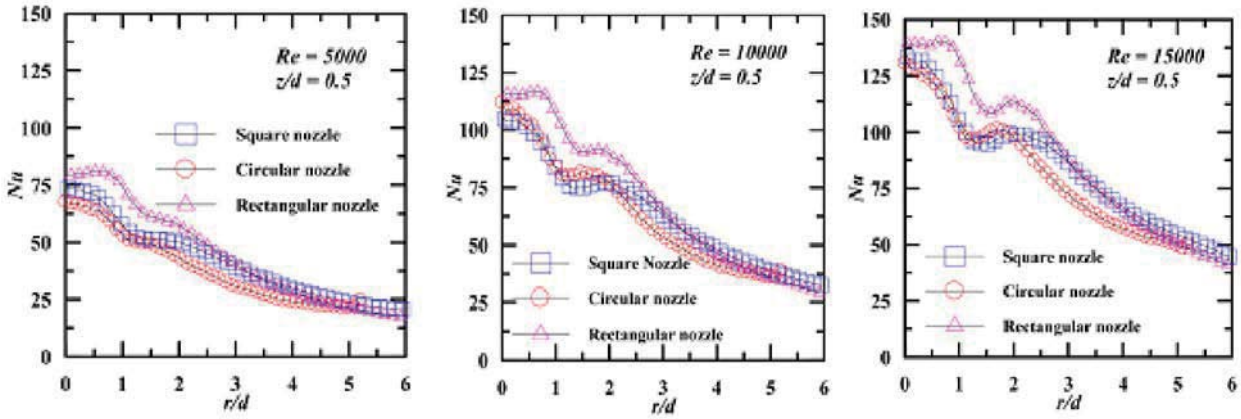

Fig. 3.1. Experimental data[4] for different Reynolds number at H/D – 0.5

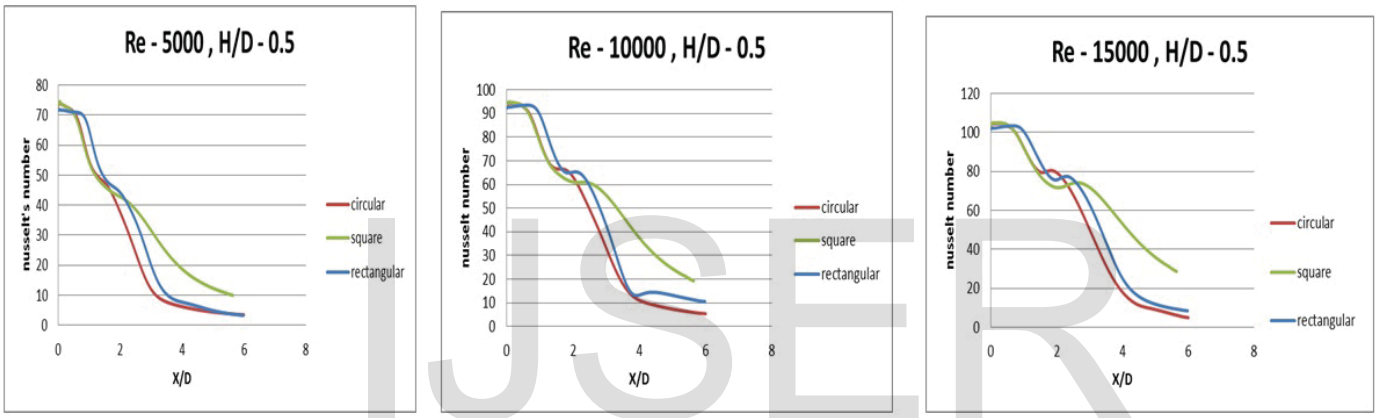

Fig. 3.2. Computational results of Nusselt number distribution for different Reynolds number at H/D – 0.5

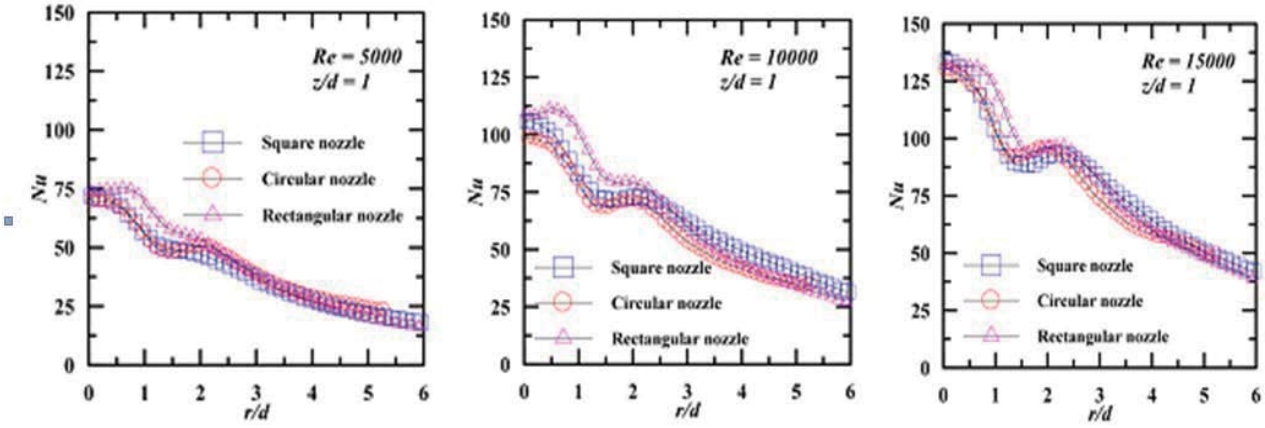

Fig. 4.1. Experimental data[4] for different Reynolds number at H/D –1

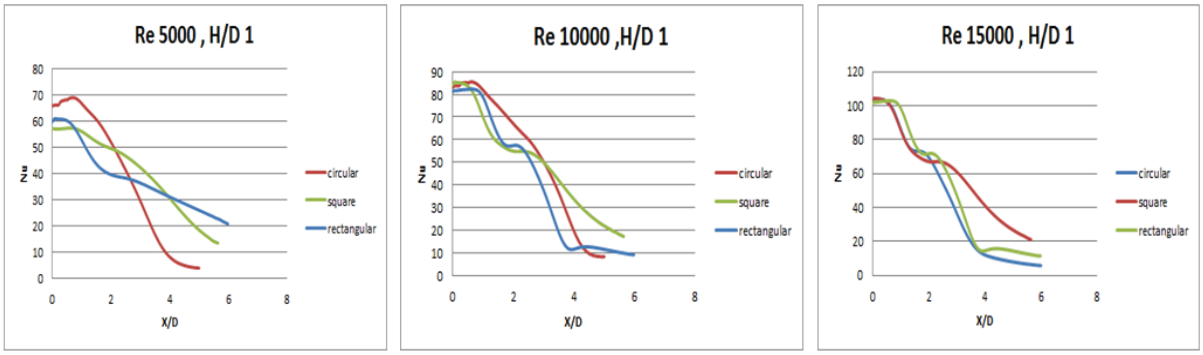

Fig. 4.2. Computational results of Nusselt number distribution for different Reynolds number at H/D –1

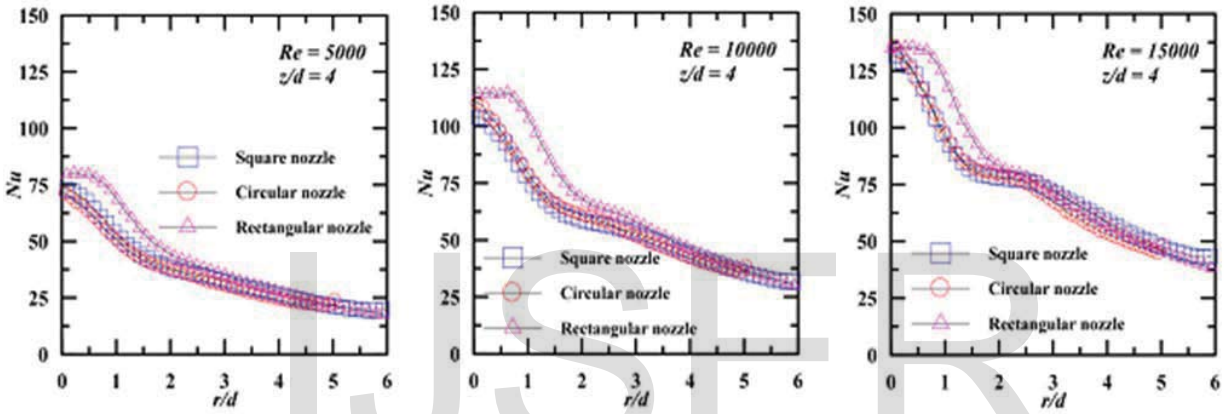

Fig. 5.1. Experimental data[4] for different Reynolds number at H/D –4

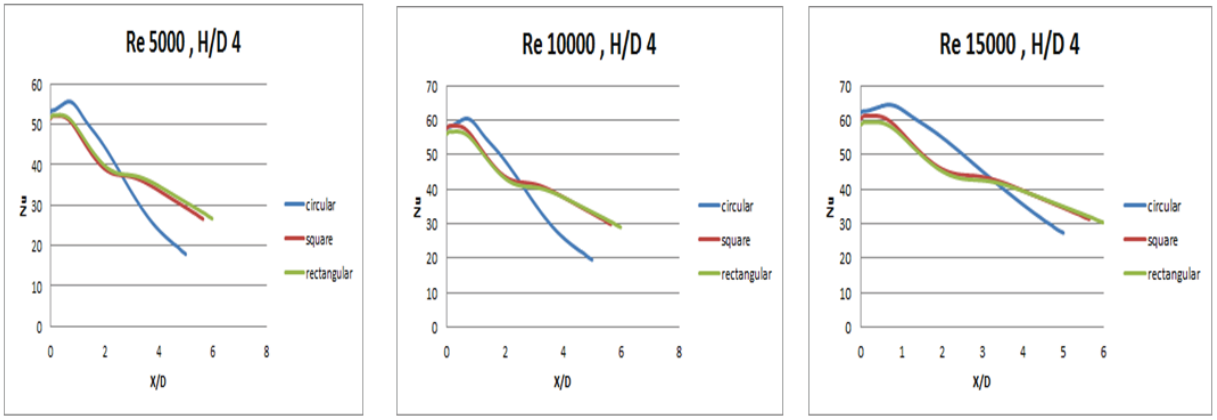

Fig. 5.2. Computational results of Nusselt number distribution for different Reynolds number at H/D –4

B. Swirl jet

Swirl flow at the nozzle exit was created by introducing four tangential inlets to the main nozzle inlet. The geometry created and the velocity contour after simulation was given in fig.6 and fig.7 respectively.

Fig.8,9 and 10 shows the heat transfer coefficient distribution of a swirl jet with constant swirl effect, impinging on a flat surface with nozzle to surface spacing 0.5 and Reynolds number 5000, 10000 and 15000.

The maximum heat transfer location shifts away considerably from the stagnation point in the radial direction due to high tangential velocity components. With the increase in Reynolds number heat transfer rate at the stagnation region decreases. This might be caused by subsidizing effect of the reduction of axial velocity by an increase in the spreading rate prior to impingement.

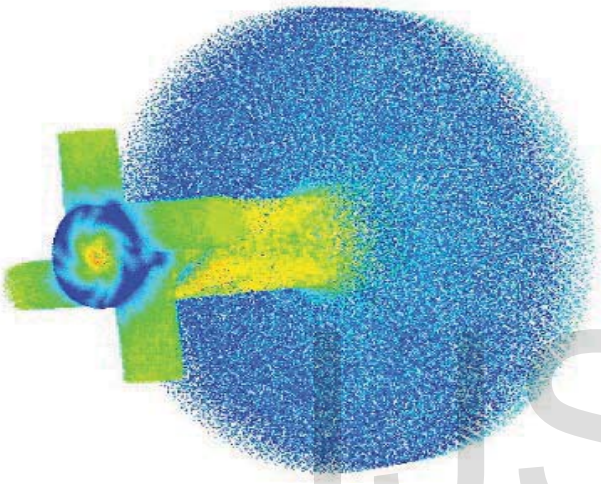

Fig.6 swirl jet nozzle geometry created in gambit after simulation

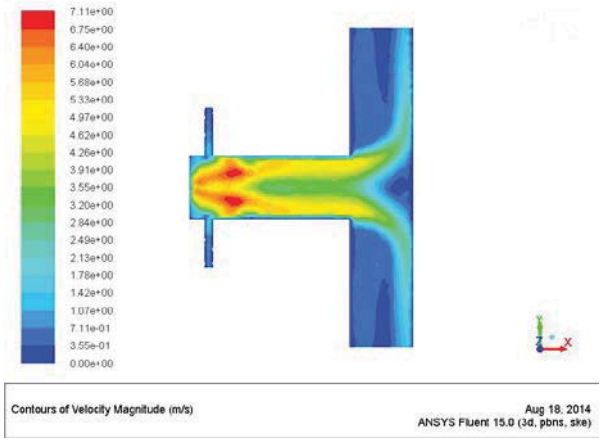

Fig.7 swirl jet velocity contour at H/d ratio 0.5

IV. CONCLUSIONS

In this study, the influence of jet inlet geometry on heat transfer characteristics of confined impinging jets has been numerically investigated. The simulations were performed for three different geometries at jet to plate spacing 0.5, 1, and 4 with Reynolds number 5000, 10000, 15000.

The major findings and conclusions derived from the present study maybe summarized as follows:

- It is observed that secondary peak diminishes as the nozzle to plate spacing increases.
- The effect of Reynolds number on the performance of non-circular jets is similar to that for the circular jet; with in-crease of Reynolds number, the heat transfer rate increases.

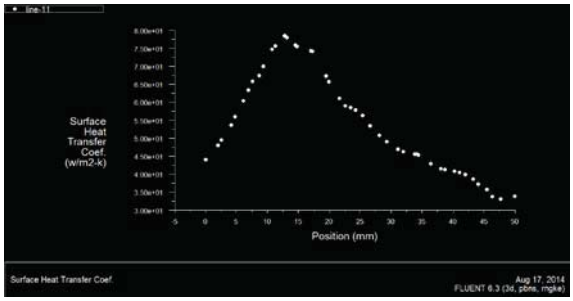

Fig. 8. Swirl jet heat transfer coefficient distribution at Re-5000

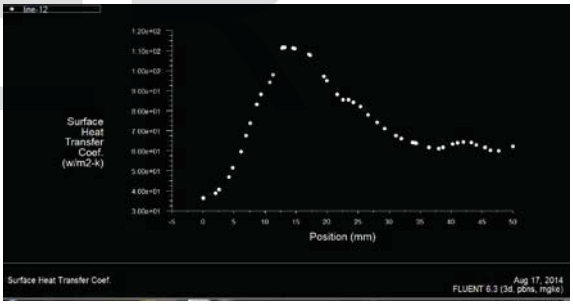

Fig. 9. Swirl jet heat transfer coefficient distribution at Re-10000

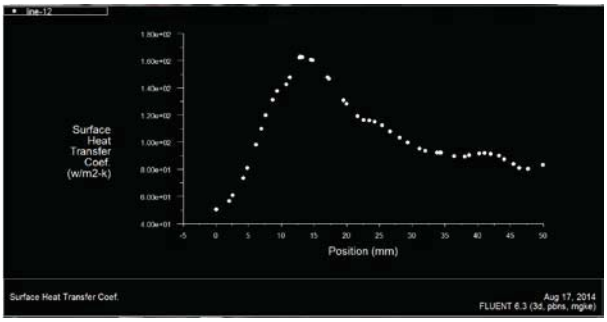

Fig. 10. Swirl jet heat transfer coefficient distribution at Re-15000

- In the stagnation region, the Nusselt number values are higher for the rectangular jet as compared to the square and the circular jet.
- For swirl jet, heat transfer rate at the stagnation region was low compared with the plain jet for same jet to plate spacing. This is due to momentum distribution of the jets before an impingement.

References

[1] Yuling shi, M.B. Ray and A.S.Mujumar, Computational study of impingement heat transfer under a turbulent slot jet, *American Chemistry Society*, 41(2002) 4643-4651

[2] M.F. Koseoglu, S. Baskaya, The role of inlet geometry in impinging jet heat transfer modeling and experiments, *International journal of Thermal Sciences*, 49(2010) 1417-1426

[3] Z.X. Yuan, Y.Y. Chen, J.G. Jiang, C.F. Ma, Swirling effect of jet impingement on heat transfer from a flat surface to CO 2 stream, *Experimental Thermal and Fluid Science* 31 (2006) 55–60

[4] Puneet Gulati, Vadiraj Katti, S.V. Prabu ,Influence of the shape of the nozzle on local heat transfer distribution between flat surface and impinging air jet, *International journal of Thermal Sciences*, 48(2009)602-617

[5] Eirik Martin Stuland, Computation of impinging gas jets, *Norwegian University of Science and Technology*, 2008.

[6] S V. Garimella, Nozzle-Geometry Effects in Liquid Jet Impingement Heat Transfer, *Heat and mass transfer* vol.39 , no.14 ,pp.2915-2923

[7] Z.Q. Lou, A.S. Mujumdar, C. Yap, Effect of geometric parameters on confined impinging jet heat transfer, Applied Thermal Science 25(2005) 2687-2697

[2] [8] S.J.Wang, A.S. Mujumdar, A comparative study of five low Reeynolds number k-ε models for impingement heat transfer, *Applied Thermal Engineering*, 25(2005) 31-44